



Article

Extreme Multistability of a Fractional-Order Discrete-Time Neural Network

A. Othman Almatroud

Department of Mathematics, Faculty of Science, University of Ha'il, Ha'il 2440, Saudi Arabia;
O.almatroud@uoh.edu.sa

Abstract: At present, the extreme multistability of fractional order neural networks are gaining much interest from researchers. In this paper, by utilizing the fractional \mathfrak{S} -Caputo operator, a simple fractional order discrete-time neural network with three neurons is introduced. The dynamic of this model are experimentally investigated via the maximum Lyapunov exponent, phase portraits, and bifurcation diagrams. Numerical simulation demonstrates that the new network has various types of coexisting attractors. Moreover, it is of note that the interesting phenomena of extreme multistability is discovered, i.e., the coexistence of symmetric multiple attractors.

Keywords: fractional neural network; chaos; multistability

MSC: 34H10; 34H15; 34D06; 37D45; 26A33



Citation: Almatroud, A.O. Extreme Multistability of a Fractional-Order Discrete-Time Neural Network.

Fractal Fract. **2021**, *5*, 202. <https://doi.org/10.3390/fractalfract5040202>

Academic Editor: Changpin Li

Received: 2 October 2021

Accepted: 28 October 2021

Published: 5 November 2021

Publisher's Note: MDPI stays neutral with regard to jurisdictional claims in published maps and institutional affiliations.



Copyright: © 2021 by the author. Licensee MDPI, Basel, Switzerland. This article is an open access article distributed under the terms and conditions of the Creative Commons Attribution (CC BY) license (<https://creativecommons.org/licenses/by/4.0/>).

1. Introduction

In one of Lorenz's studies on climatic expectation, he describes the Lorenz system [1]. Chaos has been a popular study, and many chaotic systems have been suggested during the previous 50 years. Chaotic systems are nonlinear equation systems, in which the solutions are extremely sensitive to tiny changes in the initial condition. Until recently, numerous works were devoted to studying chaotic systems defined by differential and difference equations, and have been used in a variety of disciplines, including information encryption, secure communication, economics, biology, and ecology [2]. Many special complex dynamical behaviours have also been widely studied, such as hidden attractor, coexisting, and multistability. Basically, multistability is a nonlinear dynamical system phenomenon that implies the presence of several types of attractors under varied beginning circumstances and system parameters [3,4]. It is a typical phenomenon in nonlinear systems, which has become a major source of worry for academic research committees. Because of this characteristic, chaotic systems are extremely helpful in the realm of secure communication. Coexisting bifurcations and attractors have recently been observed in discrete-time systems (maps). Multiple attractors, on the other hand, remain to be explored in the fractional-order discrete-time neural network.

According to [5,6], fractional calculus is a well-known field of mathematics that has been effectively applied in various domains of science and engineering. Discrete fractional calculus has recently become a popular research area [7,8]. Ref. [9] provided the first discrete fractional operator definition, which has been derived by discretion from a continuous-time fractional operator. Numerous different forms of difference operators were suggested over time, particularly including fractional h -difference operators, that are more extended versions of fractional difference operators [10].

Several articles on the fractional nonlinear discrete-time systems' chaotic behaviour have been published as a result of the formation of distinct discrete fractional operators. Wu and Baleanu [11] utilised the Caputo left difference operator to create a fractional version of the logistic map defined by fractional difference equations, which validated the

discrete memory. The result demonstrates that the fractional order Logistic map's complexity is proportional to the fractional order value of the systems and that it outperforms its integer equivalents. Fractional order discrete time systems with the left Caputo operator were investigated and used in a variety of disciplines since then [12–14]. Furthermore, it is demonstrated that certain systems may prevent the numerical discretization calculation error on continuous fractional systems. The fractional discrete-time systems, on the other hand, are known to exhibit more complicated dynamics than their corresponding continuous-time models.

Recently, theory and application studies of neural networks have caught widespread attention. In these artificial neural networks, the Hopfield-type neural network (HNN) is a significant nonlinear model that has played an important role [15]. In the past few years, the study of complex dynamic behaviour in the HNN has received a lot of attention in academia. Many interesting nonlinear phenomena have been discovered, such as multiple chaotic attractors and hidden attractors. Because the dynamical behaviours are closely related to the application of the HNN, a mass of modified HNN models were proposed, including fractional order HNN. As a typical non-linear behavior, chaos is observed in many fractional-order HNN models. For instance Kaslik et al., in [16], analyzed the dynamic characteristics of the fractional-order HNN; whereas in [17], bifurcation and chaos in non-integer neural networks has been illustrated. In [18], chaos and control of fractional order HNN under electromagnetic radiation was investigated. All of the above fractional-order models are continuous-time systems outlined by differential equations with fractional order. For discrete-time fractional-order HNN, there is little literature on the investigation of the chaotic behaviour [19–25]. For example, in [19], discrete fractional complex-valued HNN was synchronized without exploring the chaotic dynamics; whereas in [20], the authors studied the chaotic behavior of a 3D discrete HNN with commensurate fractional order. The main advantage of fractional-order NN in comparison with the integer-order model lies in two aspects, one is its infinite memory, the other is that the fractional-order parameter enriches the system performance by increasing one degree of freedom.

Since the phenomena of multistability in fractional-order discrete-time neural network is still unexplored, the goal of this study is to contribute to the field of fractional-order discrete-time systems by describing and analysing the dynamics of a unique 3D fractional discrete-time neural network that employs the Caputo-like difference operator. The main contribution of the paper are as follows:

- It provides a new way to describe fractional order systems resulting by replacing the Caputo fractional derivative with Caputo difference operator, without any loss in the memory effects, which leads to better results.
- It is the first fractional-order discrete-time neural network to exhibit extreme multistability, or the coexistence of several attractors given the same variety of system parameters and initial conditions.
- For different fractional order values, different coexisting behaviors of asymmetric attractors emerged under different initial conditions.
- Extreme multistability behaviors of symmetric attractors have been discovered and thoroughly explored.

The rest of the paper is organized as follows. Section 2 gives some primary preliminaries associated with discrete fractional calculus. Section 3, introduces the new three-neuron fractional-order discrete-time HNN. The dynamic properties of the conceived fractional HNN are analyzed via bifurcation diagrams, phase portrait, and maximum LE. The 3D neuron model possesses an interesting property, i.e., it is characterized by extreme multistability behaviors of symmetric attractors. In Section 4 a conclusion with potential future work is reported.

2. Preliminaries

For completeness, several preliminaries and basic ideas connected with discrete fractional calculus are provided here, before we start investigating fractional order discrete

neural network models. Fractional difference operators are defined by three various definitions: Grunwald-Letnikov, Caputo, and Riemann-Liouville operators, which have been shown to be useful in engineering applications. In the contest, we consider a function X defined from a discrete time scale \mathbb{N}_a , where $\mathbb{N}_a = \{a, a + 1, a + 2, \dots\}$ and $a \in \mathbb{R}$. The forward difference operator is represented as:

$$\Delta x(n) = x(n + 1) - x(n). \quad (1)$$

In order to give a reasonable treatment of the discrete fractional calculus, we begin by recalling Euler's Gamma function:

$$\Gamma(\mathfrak{S}) = \int_0^{\infty} s^{\mathfrak{S}} \exp^{-s}. \quad (2)$$

This function is a factorial derivation in the governing equations:

$$\Gamma(n) = (n - 1)!. \quad (3)$$

Definition 1. The falling factorial function of real order \mathfrak{S} is defined as:

$$s^{(\mathfrak{S})} = \frac{\Gamma(s + 1)}{\Gamma(s + 1 - \mathfrak{S})}. \quad (4)$$

Definition 2. In [7], the \mathfrak{S} -th fractional sum for $\Delta_{\tau}^m X(s)$ with $\mathfrak{S} > 0$, is defined by :

$$\Delta_a^{-\mathfrak{S}} X(s) = \frac{1}{\Gamma(\mathfrak{S})} \sum_{\tau=a}^{s-\mathfrak{S}} (s - \tau - 1)^{(\mathfrak{S}-1)} X(\tau). \quad (5)$$

Based on the above definition of the \mathfrak{S} -th fractional sum, it is possible to define the \mathfrak{S} -Caputo like difference operator. Let X denote any function defined from $\mathbb{N}_{a+m-\mathfrak{S}}$. The Caputo difference operator with order $\mathfrak{S} \neq \mathbb{N}$, is defined by:

Definition 3. In [10] The \mathfrak{S} -Caputo type delta difference of a function $X(s) : \mathbb{N}_a \rightarrow \mathbb{R}$, which is of the form:

$$\begin{aligned} {}^c \Delta_a^{\mathfrak{S}} X(s) &= \Delta_a^{-(m-\mathfrak{S})} \Delta^m X(s) \\ &= \frac{1}{\Gamma(m-\mathfrak{S})} \sum_{\tau=a}^{s-(m-\mathfrak{S})} (s - \tau - 1)^{(m-\mathfrak{S}-1)} \Delta_{\tau}^m X(\tau), \end{aligned} \quad (6)$$

for $\mathfrak{S} \notin \mathbb{N}$ is the fractional order, $s \in \mathbb{N}_{a+m-\mathfrak{S}}$, and $m = \lceil \mathfrak{S} \rceil + 1$.

Now a theorem is briefly summarized which will allow us to define the discrete formula of fractional order discrete-time models in the following.

Theorem 1 ([8]). For the fractional difference equation:

$$\begin{cases} {}^c \Delta_a^{\mathfrak{S}} X(s) = f(s + \mathfrak{S} - 1, X(s + \mathfrak{S} - 1)), \\ \Delta^b X(a) = X_b, \quad m = \lceil \mathfrak{S} \rceil + 1, \quad b = 0, 1, \dots, m - 1, \end{cases} \quad (7)$$

the unique solution of the initial value problem (7) is given by:

$$\begin{aligned} X(s) &= X_0(s) + \frac{1}{\Gamma(\mathfrak{S})} \sum_{\tau=a+m-\mathfrak{S}}^{s-\mathfrak{S}} (s - \sigma(\tau))^{(\mathfrak{S}-1)} \\ &\quad f(\tau + \mathfrak{S} - 1, X(\tau + \mathfrak{S} - 1)), \end{aligned} \quad (8)$$

where $s \in \mathbb{N}_{\mathfrak{S}+m}$, and:

$$X_0(s) = \sum_{b=0}^{m-1} \frac{(s-a)^{(b)}}{\Gamma(b+1)} \Delta^b X(a). \quad (9)$$

3. A Fractional Order Discrete-Time Neural Network

3.1. The Mathematical Model

Kaslik and Sivasundaram, in reference [4], discuss the stability of a fractional-order neural network of Hopfield type. The fractional-order Hopfield neural network, which is made up of n neurons, can be described by:

$${}^c D^q x_i(s) = -a_i x_i(s) + \sum_{j=1}^n T_{ij} g_j(x_j(s)) + I_i, \quad \forall s > 0 \quad (10)$$

where $T = (T_{ij})_{n \times n}$ is the synaptic weight value describing the connection between neurons i and j [22]. $a_i > 0$ are the self-regulating parameters of the neurons and $g_i : \mathbb{R} \rightarrow \mathbb{R}$ are the neurons activation functions. Besides, I_i denotes the external inputs which is equal to zero in our study. ${}^c D^q$ denotes the Caputo fractional order derivatives given by:

$${}^c D^q X(s) = \frac{1}{\Gamma(n-q)} \int_{s_0}^s (s-\tau)^{n-q-1} X^{(n)}(\tau) d\tau, \quad (11)$$

q is the fractional order $q \in (0, 1]$.

In this study, a fractional-order continuous neural network with three neurons is considered for simplicity. Assuming $a_i = 1$ and $g(x) = \sin(x_j)$, the weights matrix T can be expressed as:

$$T = \begin{pmatrix} 2 & T_1 & T_2 \\ T_2 & 2 & T_1 \\ T_1 & T_2 & 2 \end{pmatrix}.$$

This yields the following fractional order continuous neural networks:

$$\begin{cases} {}^c D^q x_1(s) = -x_1(s) + 2 \sin(x_1) + T_1 \sin(x_2) + T_2 \sin(x_3), \\ {}^c D^q x_2(s) = -x_2(s) + T_2 \sin(x_1) + 2 \sin(x_2) + T_1 \sin(x_3), \\ {}^c D^q x_3(s) = -x_3(s) + T_1 \sin(x_1) + T_2 \sin(x_2) + 2 \sin(x_3). \end{cases} \quad (12)$$

Inspired by the relevant work on fractional-order discrete time neural networks [20], we replace the continuous Caputo fractional operator ${}^c D^q$ in system (12) with the discrete Caputo like difference operator ${}^C \Delta_n^{\mathfrak{S}}$, one will obtained the corresponding fractional-order discrete-time neural network (FoDtNN):

$$\begin{cases} {}^C \Delta_n^{\mathfrak{S}} x_1(s) = -x_1(s-1+\mathfrak{S}) + 2 \sin(x_1(s-1+\mathfrak{S})) + T_1 \sin(x_2(s-1+\mathfrak{S})) + T_2 \sin(x_3(s-1+\mathfrak{S})), \\ {}^C \Delta_n^{\mathfrak{S}} x_2(s) = -x_2(s-1+\mathfrak{S}) + T_2 \sin(x_1) + 2 \sin(x_2(s-1+\mathfrak{S})) + T_1 \sin(x_3(s-1+\mathfrak{S})), \\ {}^C \Delta_n^{\mathfrak{S}} x_3(s) = -x_3(s-1+\mathfrak{S}) + T_1 \sin(x_1(s-1+\mathfrak{S})) + T_2 \sin(x_2(s-1+\mathfrak{S})) + 2 \sin(x_3(s-1+\mathfrak{S})), \end{cases} \quad (13)$$

where $s \in \mathbb{N}_{b+1-\mathfrak{S}}$ and $\mathfrak{S} \in (0, 1]$ is the fractional order. The fractional order's complicated dynamics are described in this section, and the lowest order for chaos to occur is found. We shall first give the numerical formula of the FoDtNN (13) using the criterion in Theorem 1. Take $n = s - l$, $l = 0$ and since $(s - \tau - 1)^{(\mathfrak{S}-1)}$ is equal to $\Gamma(s - \tau) / \Gamma(s - \tau - \mathfrak{S} + 1)$, it follows from Theorem 1 that:

$$\begin{cases} x_1(n) = x_1(0) + \frac{1}{\Gamma(\mathfrak{S})} \sum_{i=0}^{n-1} \frac{\Gamma(n-1-i+\mathfrak{S})}{\Gamma(n-i)} (-x_1(i) + 2 \sin(x_1(i)) + T_1 \sin(x_2(i)) + T_2 \sin(x_3(i))), \\ x_2(n) = x_2(0) + \frac{1}{\Gamma(\mathfrak{S})} \sum_{i=0}^{n-1} \frac{\Gamma(n-1-i+\mathfrak{S})}{\Gamma(n-i)} (-x_2(i) + T_2 \sin(x_1(i)) + 2 \sin(x_2(i)) + T_1 \sin(x_3(i))), \\ x_3(n) = x_3(0) + \frac{1}{\Gamma(\mathfrak{S})} \sum_{i=0}^{n-1} \frac{\Gamma(n-1-i+\mathfrak{S})}{\Gamma(n-i)} (-x_3(i) + T_1 \sin(x_1(i)) + T_2 \sin(x_2(i)) + 2 \sin(x_3(i))) \end{cases} \quad (14)$$

where $x_1(0)$, $x_2(0)$ and $x_3(0)$ are the initial states. Due to the numerical formula (14), the FoDtNN (13) has memory effect, which means that the iterated solutions $x_i(n)$ are determined by all the previous states. For $T_1 = -1$, $T_2 = 0$, and constant order $\mathfrak{S} = 0.98$ the FoDtNN (13) is chaotic. Figure 1 shows the chaotic attractor and trajectories, respectively.

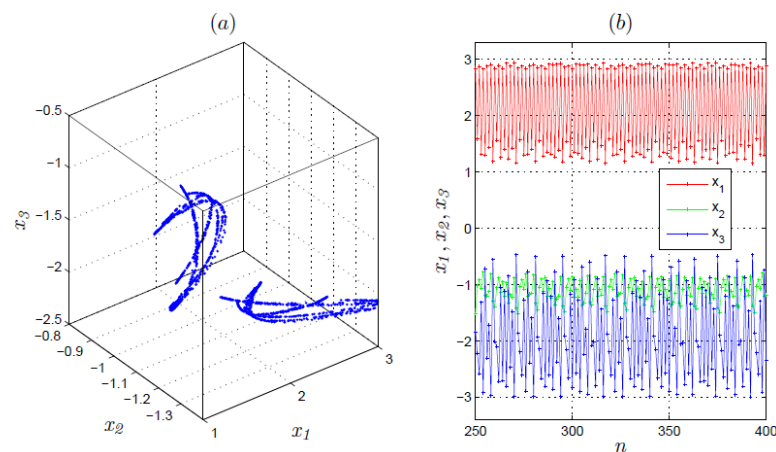


Figure 1. Chaotic attractor and trajectories of the FoDtNN (13) for the initial conditions $(x_1(0), x_2(0), x_3(0)) = (0.1, 0.1, 0.1)$, fractional order $\mathfrak{S} = 0.98$ and $T_1 = -1, T_2 = 0$. (a) Chaotic attractors, (b) chaotic trajectories x_1, x_2, x_3 .

3.2. Dynamical Analysis and Numerical Simulations

In the following, we present the dynamics of the FoDtNN (13) by considering some numerical simulation. Phase portraits, maximum Lyapunov exponents (MLEs), and bifurcation diagrams are examples of such simulations. The impact of fractional order and starting circumstances on the dynamical behaviour of the new system is studied in depth, with the goal of highlighting the coexistence of several chaotic attractors. Note that, through the manuscript, all the simulation results and related figures are obtained using the software MATLAB.

3.2.1. Coexisting of Symmetric Attractors Depending on System Parameter T_1

Obviously, the FoDtNN (13) is invariant under transformation $(x_1, x_2, x_3) \rightarrow (-x_1, -x_2, -x_3)$, for all values of parameters T_1, T_2 and fractional order \mathfrak{S} . Hence this system could display coexisting attractors for the appropriate choice of initial conditions and fractional order. In order to explore this property, the bifurcation diagrams and maximum Lyapunov exponent (MLE) are considered by changing the bifurcation parameter T_1 for $T_1 \in [-10, 10]$, when selecting the constant $T_2 = 0$. Taking symmetrical initial conditions and fractional order value $\mathfrak{S} = 0.98$, the bifurcation diagrams are plotted in Figure 2 with the maximum LE for the initial conditions $(0.1, 0.1, 0.1)$. Note that the bifurcation diagram in blue starts with the initial conditions $(x_1(0), x_2(0), x_3(0)) = (0.1, 0.1, 0.1)$, while the bifurcation diagram in red begins with the initial conditions $(x_1(0), x_2(0), x_3(0)) = (-0.1, -0.1, -0.1)$. As can be seen, the neural network (13) exhibits extremely complex dynamics behavior including, chaos, periodic windows, period doubling bifurcation, and coexisting attractors. When the value of T_1 increases the FoDtNN (13) has multiple internal crises points. Moreover, it can be obtained from the MLE diagram in Figure 2, that when $T_1 \in [-9.675, -7.192] \cup [-6.625, -3.26] \cup [-2.722, -1] \cup [1, 10]$ the system (13) is in chaos with some periodic windows where the maximum LE is positive and fits well with the coexisting bifurcation diagrams. In particular, symmetric coexisting attractors are observed in the interval $[-1, 1.6]$, i.e., coexisting chaotic attractors, coexisting period-two, and period-four attractors. To observe the coexisting region better, a close look to the bifurcation diagram in the interval $[-3, 3]$ is provided in Figure 3.

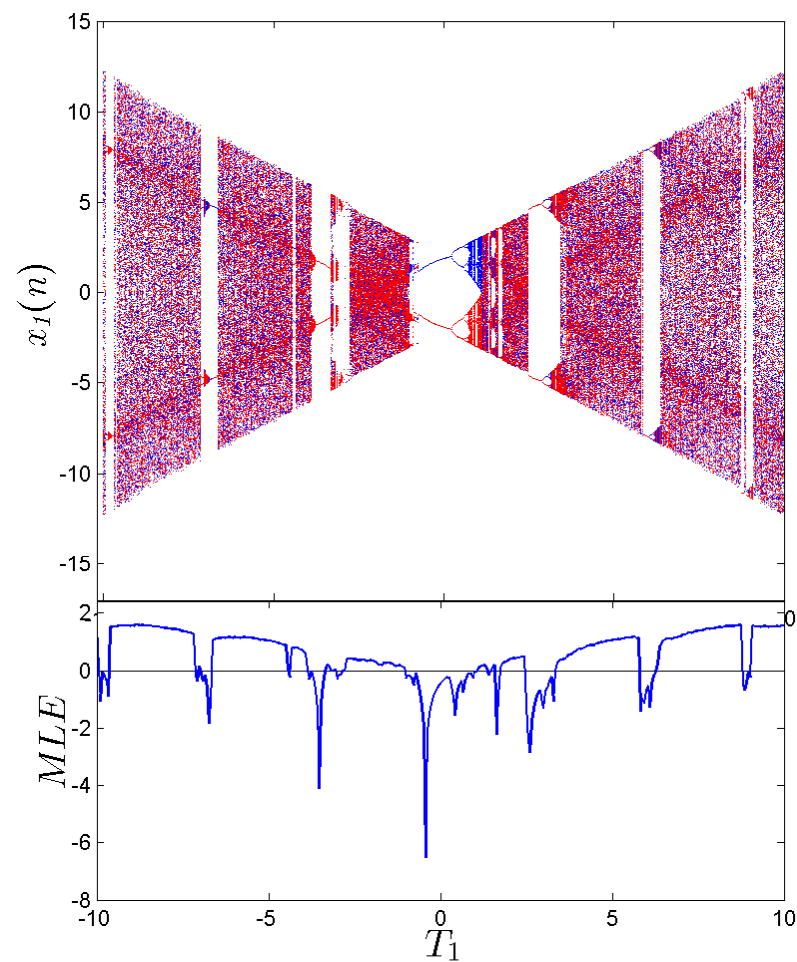


Figure 2. Bifurcation diagrams and maximum Lyapunov exponents of the fractional-order discrete-time neural network (13) versus T_1 for fractional order value $\mathfrak{S} = 0.98$, system parameter $T_2 = 0$ and a set of symmetric initial conditions: $(0.1, 0.1, 0.1)$ blue diagram, $(-0.1, -0.1, -0.1)$ red diagram.

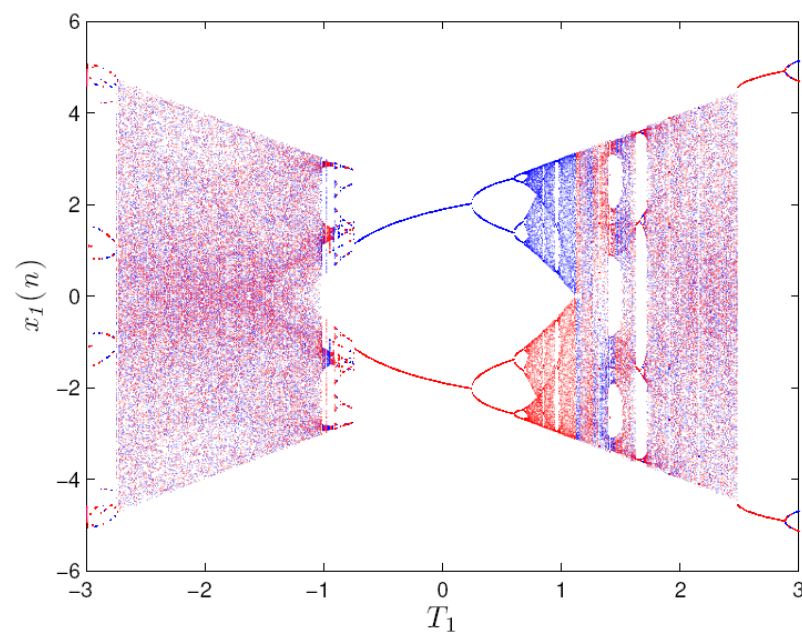


Figure 3. Coexisting dynamics of the FoDtNN (13) with respect to the bifurcation parameter $T_1 \in [-3, 3]$ for fractional order value $\mathfrak{S} = 0.98$ and symmetric initial condition $(\pm 0.1, \pm 0.1, \pm 0.1)$.

Two phase portraits of coexisting symmetric attractors with different parameters T_1 are presented in Figure 4, where the red trajectories are obtained for the initial conditions $(-0.1, -0.1, -0.1)$; while the blue trajectories are obtained for $(0.1, 0.1, 0.1)$.

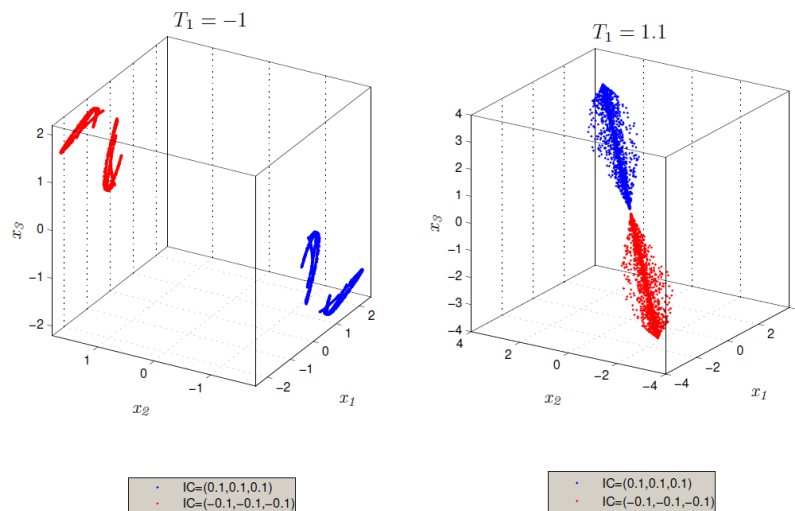


Figure 4. Two coexisting chaotic attractors for the symmetrical initial conditions $(\pm 0.1, \pm 0.1, \pm 0.1)$, fractional order $\mathfrak{S} = 0.98$ where positive initial conditions in blue trajectories, and negative system parameters in red trajectories with $T_2 = 0$.

3.2.2. Coexisting Symmetric Attractors Depending on the Fractional Order \mathfrak{S}

To further investigate the dynamics of the FoDtNN (13), the relationship between the state variable and the fractional order \mathfrak{S} , and computations of maximum LEs with respect to the fractional order are carried out. We choose to change the fractional order value \mathfrak{S} from 0 to 1 while the bifurcation parameters are fixed. Figure 5 displays the bifurcation diagrams of the state variable x_1 corresponding to the system parameters $T_1 = -1$, $T_2 = 0$ and positive initial condition $(0.1, 0.1, 0.1)$ in the blue diagram and the negative initial condition $(-0.1, -0.1, -0.1)$ in the red diagram. The corresponding maximum LE diagram is presented in Figure 5 with $n = 5000$. Figure 5 shows that the states of the proposed neural network goes from chaos to periodic states and then to limit circles with some periodic windows as the order \mathfrak{S} decreases. Furthermore, it is deduced that the FoDtNN (13) exhibits coexisting chaotic and periodic attractors. To illustrate more of these properties, we choose to plot the phase portraits of the 3D FoDtNN for two symmetric initial conditions $(\pm 0.1, \pm 0.1, \pm 0.1)$ and for six fractional order values with $T_1 = -1$ and $T_2 = 0$. The obtained results are plotted in Figure 6. When $\mathfrak{S} = 0.95$ and $\mathfrak{S} = 0.846$, there are two symmetric separate chaotic attractors, while two periodic attractors coexisted for $\mathfrak{S} = 0.08$ and $\mathfrak{S} = 0.51$.

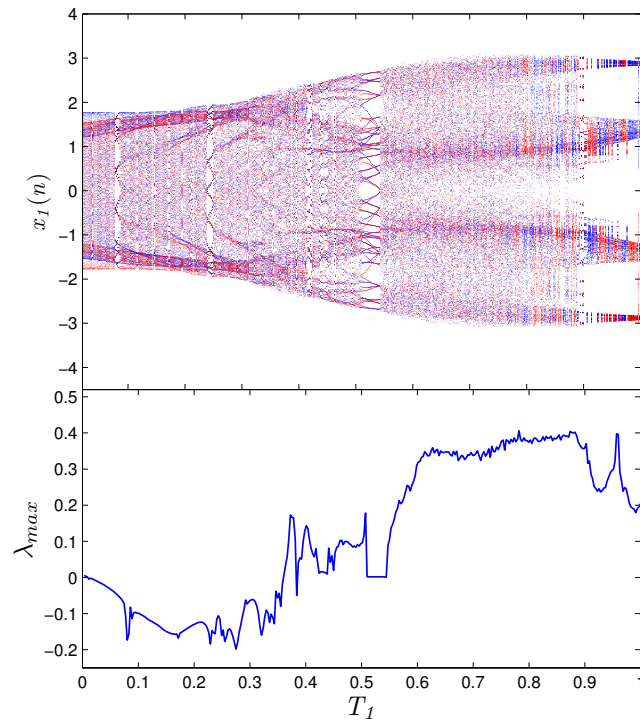


Figure 5. Bifurcation diagrams and maximum Lyapunov exponents of the fractional-order discrete-time neural network (13) versus fractional order \mathfrak{S} for system parameters $T_1 = -1, T_2 = 0$ and a set of symmetric initial conditions: $(0.1, 0.1, 0.1)$ blue diagram, $(-0.1, -0.1, -0.1)$ red diagram.

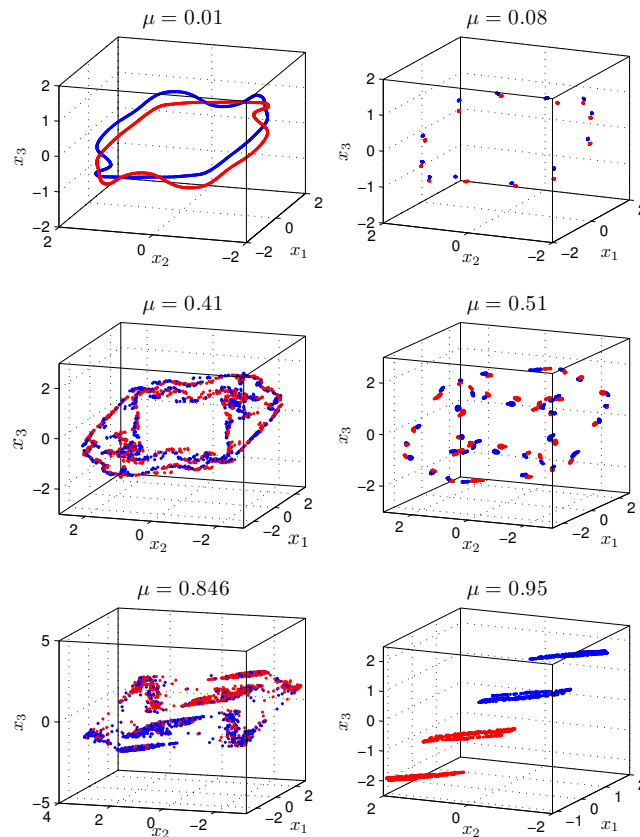


Figure 6. Some coexisting symmetric attractors for different fractional order values and parameters $T_1 = -1, T_2 = 0$ and two symmetric initial conditions: $(0.1, 0.1, 0.1)$ blue attractors, $(-0.1, -0.1, -0.1)$ blue attractors.

3.2.3. Extreme Multistability Analysis

In order to reveal the extreme multistability phenomena of the FoDtNN (13), the maximum LEs and bifurcation diagrams of the state variable x_3 are calculated as shown in Figures 7 and 9, where the fractional order \mathfrak{S} are chosen as 0.98 and 0.1, respectively. The parameters are selected as $T_1 = -1$ and $T_2 = 0$, and the initial conditions are fixed as $x_1(0) = x_2(0) = 0.1$, while $x_3(0)$ is varied from -20 to 20 . As shown in Figure 7, when $\mathfrak{S} = 0.98$, system (13) generates multiple chaotic attractors along the x_3 axis, where the values of the LEs of the FoDtNN (13) are nearly the same, which indicates that all these attractors have very close chaotic features. For the sake of exhibiting the phenomenon of multistability, typical chaotic attractors of the network (13) for different initial condition $x_3(0)$ are simulated, as shown in Figure 8. In the same way, Figure 9 displays the phenomena of extreme multistability, i.e., the coexisting of many attractors. From Figure 9, when $\mathfrak{S} = 0.1$ the fractional neural network states changes from stable states to periodic states, then to chaos via the period doubling bifurcation route. Obviously, the dynamic behaviour of the FoDtNN (13) depends on the initial condition and the value of \mathfrak{S} . For simplicity, two phase portraits of the attractors in the 3D plane are displayed in Figure 10. In particular, Figure 10 reveals the periodic attractor for the initial state $(0.1, 0.1, 0.1)$ and the chaotic attractor for the initial state $(0.1, 0.1, -10)$. These previous figures confirm the rich dynamics of the proposed fractional order discrete-time neural network, illustrating that several attractors might be identified by using different $x_3(0)$ quantities as well as various fractional order numbers in the $\mathfrak{S} \in (0, 1]$ range.

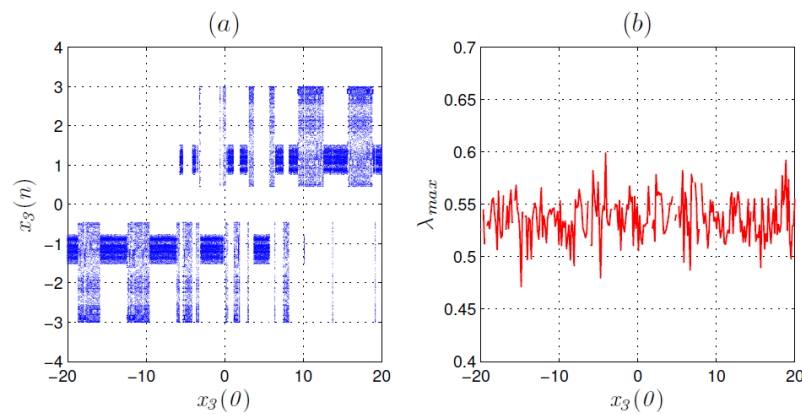


Figure 7. (a) Bifurcation diagram and maximum LEs of FoDtNN (13) versus (b) initial condition $x_3(0)$, for parameter values $T_1 = -1$, $T_2 = 0$, and fractional order $\mathfrak{S} = 0.98$.

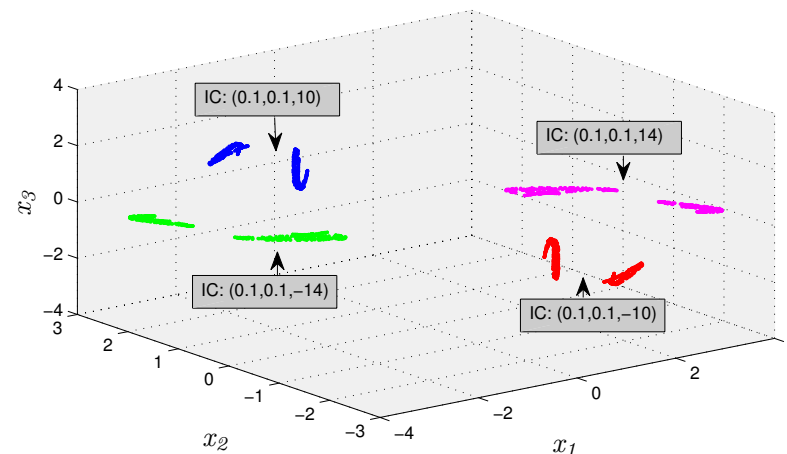


Figure 8. For coexisting chaotic attractors for different initial condition values $x_3(0)$ and system parameters $T_1 = -1$, $T_2 = 0$, and fractional order $\mathfrak{S} = 0.98$.

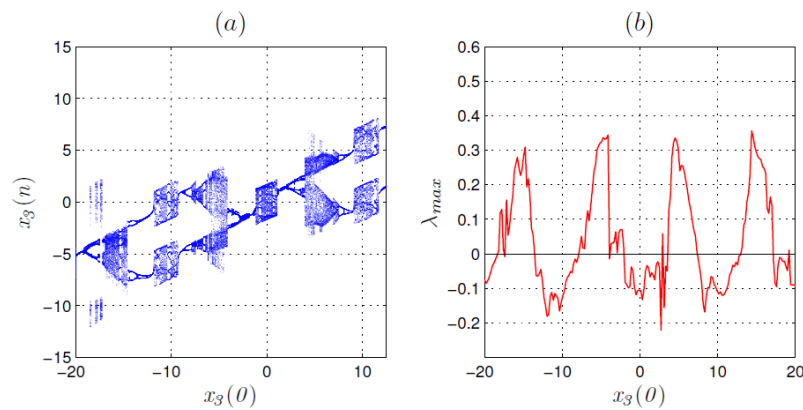


Figure 9. (a) Bifurcation diagram and maximum LEs of the FoDtNN (13) versus (b) initial condition $x_3(0)$, for parameter values $T_1 = -1$, $T_2 = 0$, and fractional order $\mathfrak{S} = 0.1$.

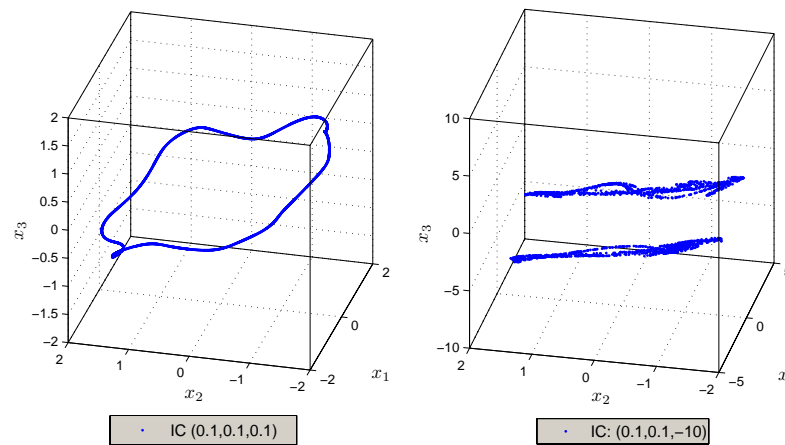


Figure 10. Two phase portraits of the FoDtNN (13) for fractional order $\mathfrak{S} = 0.1$, initial condition $x_1 = x_2 = 0.1$. Periodic attractor for $x_3 = 0.1$, chaotic attractor for $x_3 = -10$.

4. Conclusions

Referring to fractional-order discrete-time neural networks, this paper has introduced a new FoDtNN with an extreme multistability property. The conceived network has shown the existence of different types of symmetric chaotic attractors. Dynamics of the conceived network have been analyzed in details via bifurcation diagrams and maximum Lyapunov exponents. Compared with the network with memory effects, the fractional network with short memory and variable order has more complexity. Due to the rich complex dynamical behaviour, this research can provide a theoretical basis and help for research in the encryption field and secure communication.

Funding: I declare that funding is not applicable for this paper.

Institutional Review Board Statement: Not applicable.

Informed Consent Statement: Not applicable.

Data Availability Statement: Not applicable.

Conflicts of Interest: The author declares no conflict of interest.

References

1. Lorenz, E.N.; Lorenz, F.N. *The Nature and Theory of the General Circulation of the Atmosphere*; World Meteorological Organization: Geneva, Switzerland, 1967.
2. Lazaros, M.; Eleftherios, P.; Christos, V.; Hector, N.; Ioannis, S. A chaotic path planning generator based on logistic map and modulo tactics. *Robot. Auton. Syst.* **2020**, *124*, 103377.

3. Guangyi, W.; Chuanbao, S.; Xiaowei, W.; Fang, Y. Coexisting oscillation and extreme multistability for a memcapacitor-based circuit. *Math. Probl. Eng.* **2017**, *2017*, 6504969.
4. Kaslik, E.; Sivasundaram, S. Dynamics of Fractional-Order Neural Networks. In Proceedings of the International Joint Conference on Neural Networks, San Jose, CA, USA, 31 July–5 August 2011.
5. Podlubny, I. *Fractional Differential Equations: An Introduction to Fractional Derivatives, Fractional Differential Equations, to Methods of Their Solution and Some of Their Applications*; Elsevier: Amsterdam, The Netherlands, 1999.
6. Ostalczyk, P. *Discrete Fractional Calculus: Applications in Control and Image Processing*; World Scientific: Singapore, 2015.
7. Atici, F.M.; Eloe, P. Discrete fractional calculus with the nabla operator. *Electron. J. Qual. Theory Differ. Equ.* **2009**, *3*, 1–12.
8. Anastassiou, G.A. Principles of delta fractional calculus on time scales and inequalities. *Math. Comput. Model.* **2010**, *52*, 556–566. [[CrossRef](#)]
9. Diaz, J.B.; Osler, T.J. Differences of fractional order. *Math. Comput.* **1974**, *125*, 185–202. [[CrossRef](#)]
10. Abdeljawad, T. On Riemann and Caputo fractional differences. *Comput. Math. Appl.* **2011**, *62*, 1602–1611. [[CrossRef](#)]
11. Wu, G.C.; Dumitru, B. Discrete fractional logistic map and its chaos. *Nonlinear Dyn.* **2014**, *75*, 283–287. [[CrossRef](#)]
12. Ouannas, A.; Khennaoui, A.A.; Odibat, Z.; Pham, V.T.; Grassi, G. On the dynamics, control and synchronization of fractional-order Ikeda map. *Chaos Solitons Fractals* **2019**, *123*, 108–115. [[CrossRef](#)]
13. Khennaoui, A.A.; Ouannas, A.; Bendoukha, S.; Grassi, G.; Lozi, R.P.; Pham, V.T. On Fractional Order Discrete Time Systems: Chaos, Stabilization and Synchronization. *Chaos Solitons Fractals* **2019**, *119*, 150–162. [[CrossRef](#)]
14. Khennaoui, A.A.; Ouannas, A.; Bendoukha, S.; Grassi, G.; Wang, X.; Pham, V.T.; Alsaadi, F.E. Chaos, control, and synchronization in some fractional-order difference equations. *Adv. Differ. Equ.* **2019**, *1*, 1–23. [[CrossRef](#)]
15. Hopfield, J.J. Neuron with graded response have computational properties like those of two-state neurons. *Proc. Natl. Acad. Sci. USA* **1984**, *81*, 3088–3092. [[CrossRef](#)]
16. Kaslik, E.; Radulescu, I.R. Dynamics of complex-valued fractional-order neural networks. *Neural Netw.* **2017**, *89*, 39–49. [[CrossRef](#)]
17. Arena, P.; Caponetto, R.; Fortuna, L.; Porto, D. Bifurcation and chaos in noninteger order cellular neural networks. *Int. J. Bifurc. Chaos* **1998**, *8*, 1527–1539. [[CrossRef](#)]
18. Allehiyany, F.M.; Mahmoud, E.E.; Jahanzaib, L.S.; Trikha, P.; Alotaibi, H. Chaos control and analysis of fractional order neural network under electromagnetic radiation. *Results Phys.* **2021**, *21*, 103786. [[CrossRef](#)]
19. You, X.; Song, Q.; Zhao, Z. Global Mittag-Leffler stability and synchronization of discrete-time fractional-order complex-valued neural networks with time delay. *Neural Netw.* **2020**, *122*, 382–394. [[CrossRef](#)]
20. Chen, L.; Hao, Y.; Huang, T.; Yuan, L.; Zheng, S.; Yin, L. Chaos in fractional-order discrete neural networks with application to image encryption. *Neural Netw.* **2020**, *125*, 177–184. [[CrossRef](#)]
21. Wu, G.C.; Luo, M.; Huang, L.L.; Banerjee, S. Short memory fractional differential equations for new memristor and neural network design. *Nonlinear Dyn.* **2020**, *100*, 3611–3623. [[CrossRef](#)]
22. Lin, H.; Wang, C.; Yao, W.; Tan, Y. Chaotic dynamics in a neural network with different types of external stimuli. *Commun. Nonlinear Sci. Numer. Simulat.* **2020**, *90*, 105390. [[CrossRef](#)]
23. Wu, G.C.; Deng, Z.G.; Baleanu, D.; Zeng, D.Q. New variable-order fractional chaotic systems for fast image encryption. *Chaos* **2019**, *29*, 083103. [[CrossRef](#)] [[PubMed](#)]
24. Khennaoui, A.A.; Almatroud, A.O.; Ouannas, A.; Al-sawalha, M.M.; Grassi, G.; Pham, V.T.; Batiha, I.M. An Unprecedented 2-Dimensional Discrete-Time Fractional-Order System and Its Hidden Chaotic Attractors. *Math. Probl. Eng.* **2021**, *2021*, 6768215. [[CrossRef](#)]
25. Zhang, S.; Zeng, J.; Wang, X.; Zeng, Z. A novel no-equilibrium HR neuron model with hidden homogeneous extreme multistability. *Chaos Solitons Fractals* **2021**, *145*, 110761. [[CrossRef](#)]